



Colorimetric estimation of human glucose level using γ -Fe₂O₃ nanoparticles: An easily recoverable effective mimic peroxidase



Kamala Mitra^b, Abhisek Brata Ghosh^a, Arpita Sarkar^a, Namrata Saha^a, Amit Kumar Dutta^{a,*}

^a Department of Chemistry, Indian Institute of Engineering Science and Technology, Shibpur, Howrah 711 103, West Bengal, India

^b Department of Chemistry, Prasanta Chandra Mahalanobis Mahavidyalaya, 111/3 B.T.Road, Kolkata 700108, India

ARTICLE INFO

Article history:

Received 9 June 2014

Available online 11 July 2014

Keywords:

γ -Fe₂O₃ nanoparticles

Peroxidase-like activity

Hydrogen peroxide

Colorimetric glucose determination

Human blood-urine

ABSTRACT

This article reports simple, green and efficient synthesis of γ -Fe₂O₃ nanoparticles (NPs) (maghemite) through single-source precursor approach for colorimetric estimation of human glucose level. The γ -Fe₂O₃ NPs, having cubic morphology with an average particle size of 30 nm, exhibited effective peroxidase-like activity through the catalytic oxidation of peroxidase substrate 3,3',5,5'-tetramethylbenzidine (TMB) in the presence of H₂O₂ producing a blue-colored solution. On the basis of this colored-reaction, we have developed a simple, cheap, highly sensitive and selective colorimetric method for estimation of glucose using γ -Fe₂O₃/TMB/glucose–glucose oxidase (GOx) system in the linear range from 1 to 80 μ M with detection limit of 0.21 μ M. The proposed glucose sensor displays faster response, good stability, reproducibility and anti-interference ability. Based on this simple reaction process, human blood and urine glucose level can be monitored conveniently.

© 2014 Elsevier Inc. All rights reserved.

1. Introduction

Glucose is the most abundant carbohydrate, and more specifically, monosaccharide found in both plants and animals. High or low level of glucose concentration from 80 to 120 mg/dL (4.4–6.6 mM) [1–3] in human blood causes serious disease known as hyper- and hypo-glycemia, respectively. According to the World Health Organization, over 150 million people in the world were affected with diabetes in the year 2004 and it is expected to climb further to 366 million in 2030. So the patients must reduce disease-associated complications through the tight control of blood glucose levels [4]. So, convenient detection and quantitative determination of glucose are of practical importance and affected population has to be tested for blood glucose levels daily for an effective treatment. The presence of glucose in urine is also more dangerous for human body, as it is an indication of worsening of diabetes. In order to avoid the inconveniences caused by drawing blood intravenously or by hand pricking, a preliminary screening of the patients with high level diabetes (having renal glycosuria) [5,6] can be done instantly by checking their urine glucose levels.

Several analytical techniques are developed to measure glucose concentrations such as fluorescence spectroscopy [7], near infrared spectroscopy [8], Raman spectroscopy [9], nuclear magnetic resonance spectroscopy [10], liquid chromatography–mass

spectroscopy [11], high performance liquid chromatography [12], capillary electrophoresis [13], polarography [14] and electrochemical methods [15–19]. Among all these analytical techniques, colorimetric method has received considerable attention owing to their simplicity, improved sensitivity and high selectivity. Moreover this method can be interpreted by the naked eyes and involves naturally occurring peroxidase enzyme, horse-radish peroxidase (HRP) [20,21]. But HRP suffers some serious disadvantages due to lack of stability, difficult to produce in large quantities and are easily denatured in strong acidic, basic medium and high temperature. Therefore, the fabrication of efficient mimics of HRP has been an increasingly important focus for the scientists and various peroxidase mimics such as inorganic transition metal complexes [22], carbon nanotubes [23], carboxyl-modified graphene oxide [24], Fe₃O₄ nanoparticles [25], Graphene oxide–Fe₃O₄ [26], CoFe layered double hydroxide (CoFe-LDHs) nanoplates [27], Au nanoparticles [28], AuNPs (H₂O₂ triggered sol–gel transition) [29] e.t.c. have been applied for colorimetric determination of glucose. Recently, Gao et al. [20] reported that Fe₃O₄ NPs have an intrinsic enzyme mimetic activity similar to that of HRP, which opened the door for the development of nano-scaled inorganic materials in the biochemical field. However details studies on colorimetric glucose determination even in human urine using very simple, cost effective, environmental-friendly γ -Fe₂O₃ NPs has not been explored. On the other hand, this inorganic nanomaterial is easy to obtained, cheap and more stable over wide range of pH and temperature.

* Corresponding author. Tel.: +91 3326684561x512; fax: +91 3326682916.

E-mail address: amtdutta@rediffmail.com (A.K. Dutta).

In this work, we have synthesized γ -Fe₂O₃ NPs and were tested as peroxidase-mimetic through the catalytic oxidation of peroxidase substrate, TMB, in the presence of H₂O₂. Based on peroxidase catalytic activity of the NPs, we have designed a very simple and cheap colorimetric method for determination of glucose in human blood and urine. The possible pathway of the glucose catalytic process has been investigated.

2. Materials and methods

2.1. Materials

All the reagents are of analytical purity grade and have been received from commercial sources. Fe(NO₃)₃·9H₂O, ClCH₂COOH, NaHCO₃, Na₂HPO₄·2H₂O, orthophosphoric acid, anhydrous sodium acetate, acetic acid, dimethyl sulfoxide (DMSO), terephthalic acid and NaOH were purchased from commercial sources. 3,3',5,5'-tetramethylbenzidine (TMB), hydrogen peroxide (30%), D-(+)-glucose, glucose oxidase (from *Aspergillus niger*, GOx), uric acid (UA), ascorbic acid (AA), L-cysteine were purchased from Sigma–Aldrich. De-ionized water was used to prepare the solutions throughout the experiments. Acetate buffer solutions (0.1 M) with various pH were prepared by mixing stock standard solutions of sodium acetate and adjusted the pH with acetic acid or NaOH. Normal human blood as well as urine were chosen as real samples for the determination of glucose in it and were subsequently used after suitable dilution with phosphate buffer solution (PBS, pH 7.0) to reduce the matrix complexity. Solvents were used as received. The precursor complex, [Fe₃(μ₃-O)(O₂CCH₂Cl)₆(H₂O)₃]NO₃·H₂O has already been synthesized and characterized in our previous report [30].

2.2. Preparation of γ -Fe₂O₃ NPs

440 mg precursor complex [Fe₃(μ₃-O)(O₂CCH₂Cl)₆(H₂O)₃]NO₃·H₂O [30] as taken in a quartz boat, placed inside a quartz tube and was put in a horizontal tubular furnace. The complex was heated under flow of nitrogen at 440 °C and kept at that temperature for 1 h. After that the furnace was turned off and the product was cooled to room temperature under the steady stream of nitrogen.

2.3. Peroxidase-like activity measurements

The peroxidase-like behavior of the γ -Fe₂O₃ NPs was investigated spectrophotometrically through the catalytic oxidation of the peroxidase substrate TMB in presence of H₂O₂. To examine the capability of γ -Fe₂O₃ NPs as catalyst on the oxidation of TMB, 2.4 μL of 0.125 M TMB (dissolved in DMSO) in 3.0 mL NaOAc buffer (0.1 M, pH 4.0) was successively treated with (i) 20 μg γ -Fe₂O₃ NPs only, (ii) 4 μL of 30% H₂O₂ only, (iii) 4 μL of 30% H₂O₂+20 μg γ -Fe₂O₃ NPs. All the reactions were monitored spectrophotometrically in time-scan mode at 653 nm. The kinetic analysis with TMB as the substrate was performed using 20 μg γ -Fe₂O₃ NPs with fixed concentration of H₂O₂ (13 mM) and varying concentration of TMB (0, 8.3, 10.4, 14.4, 20, 40, 60, 80, 120, 160 and 200 μM). Similarly, the kinetic analysis with H₂O₂ as the substrate was performed using 20 μg γ -Fe₂O₃ NPs with fixed concentration of TMB (100 μM) and varying concentration of H₂O₂ (0, 6.5, 9.8, 13, 16, 19, 26, 32, 39, 48, 58 and 68 mM). In each case, before absorbance spectra measurement, the γ -Fe₂O₃ NPs were removed from the reaction solution by an external magnetic field. Apparent kinetic parameters were calculated based on the Michaelis–Menten equation [30].

2.4. Colorimetric glucose measurements

Glucose detection was performed as follows: (a) 20 μL of 20 mg/mL glucose oxidase (GOx) and 200 μL of D-glucose with

different concentrations in 10 mM phosphate buffer solution (PBS, pH 7.0) were incubated at 40 °C for 40 min; (b) 2.4 μL of 0.125 M TMB, 20 μL of 5 mg/mL γ -Fe₂O₃ NPs and 2 mL of 0.1 M acetate buffer (pH 4.0) were added into the above 220 μL GOx-glucose reaction system; (c) the mixed solution was incubated at 40 °C for 15 min to terminate the reaction; (d) the γ -Fe₂O₃ NPs were then removed from the reaction solution by an external magnetic field; (e) the resulting solution was used to perform the absorption spectroscopy measurement.

In order to investigate the mechanism of the glucose catalytic reaction where hydroxyl radical may be produced from the decomposition of H₂O₂, the commonly used terephthalic acid (TA) photoluminescence probing technique [31] was adopted. In this experiment, 2 × 10^{−3} M sodium terephthalate, 0.045 M glucose, 3 mL of 20 mg/mL GOx in aqueous PBS (0.01 M, pH 7.00) and three different amounts (0.15 and 25 mg) of γ -Fe₂O₃ NPs were incubated at 40 °C for 10 h. Then the luminescence spectrum was measured between 330 and 540 nm using 315 nm as the excitation wavelength.

2.5. Determination of glucose in real sample using γ -Fe₂O₃ NPs

The blood and urine samples were collected from a normal healthy male volunteer. For glucose determination in blood, the collected samples were centrifuged at 12,000 rpm for 40 min. After that, the supernatants were diluted with PBS (0.01 M, pH 7.0) before subsequent use. These diluted supernatants were then used with GOx for glucose catalyzed reaction as stated above instead of glucose aqueous solution and the corresponding absorbance values were measured at a wavelength of 653 nm. Similarly the collected urine samples were diluted with PBS (0.01 M, pH 7.0) and continued spectrophotometric measurements as stated above with GOx. Reference determinations were made by standard GOD-POD or hexokinase method in pathological laboratory.

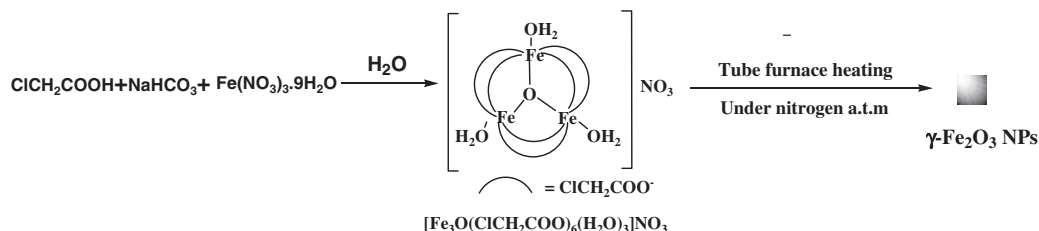
3. Results and discussion

3.1. Synthesis and characterization of the γ -Fe₂O₃ NPs

The γ -Fe₂O₃ NPs were synthesized according to Scheme 1 through simple thermal decomposition of the single source precursor complex [Fe₃(μ₃-O)(O₂CCH₂Cl)₆(H₂O)₃]NO₃·H₂O at 440 °C which was synthesized by reacting Fe(NO₃)₃·9H₂O with two equivalents of chloroacetic acid, previously neutralized by NaHCO₃, in aqueous medium according to our previous report [30]. The thermogravimetric analysis (TGA) of the precursor complex (Fig. S1) revealed that the total weight loss agrees satisfactorily for the formation of Fe₂O₃ as the final product.

The crystallinity and phase purities of the Fe₂O₃ NPs were first examined by the X-ray diffraction (XRD) technique. The diffraction pattern of the crystalline product (Fig. 1A) matches quite well with the standard diffraction data for the pure primitive phase of cubic maghemite (Fe₂O₃) (JCPDS ID. 391346). In Fig. 1A, the peaks at 2θ values of 30.18, 35.54, 43.26, 53.67, 57.24 and 62.84 can be indexed to the (220), (311), (400), (422), (511) and (440) planes of Fe₂O₃, respectively. The relative broad feature of the peaks (FWHM) indicates the presence of smaller crystallites. The average grain size of the NPs, as calculated by the Debye–Scherrer equation ($D = 0.9\lambda/(\beta \cos \theta)$), where D is the crystallite size (diameter), λ the wave length of X-ray ($\lambda = 1.540598$ Å), β the value of FWHM of the most intense peak (after correcting the instrumental broadening) and θ the Bragg's angle, was found to be around 24 nm.

The size and morphology of the powder material was also analyzed by transmission electron microscopy (TEM). Typical TEM image (Fig. 1B(i)) illustrates that the sample is composed of simple



Scheme 1. Synthesis of single source precursor complex $[\text{Fe}_3(\mu_3\text{-O})(\text{O}_2\text{CCH}_2\text{Cl})_6(\text{H}_2\text{O})_3]\text{NO}_3 \cdot \text{H}_2\text{O}$ and $\gamma\text{-Fe}_2\text{O}_3$ nanoparticles.

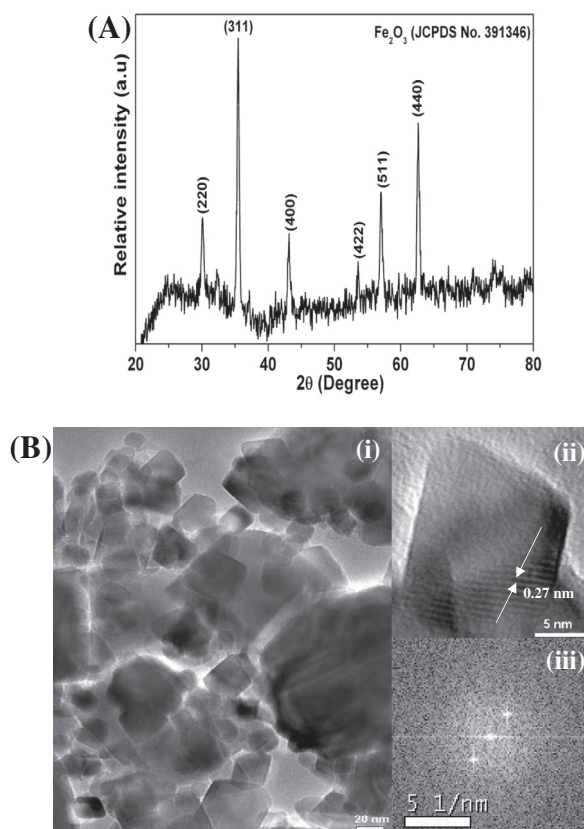


Fig. 1. (A) Powder XRD pattern of $\gamma\text{-Fe}_2\text{O}_3$ NPs and (B) (i) TEM (ii) HRTEM and (iii) Live FFT image of $\gamma\text{-Fe}_2\text{O}_3$ NPs.

cubic $\gamma\text{-Fe}_2\text{O}_3$ with an average particle size of about 30 nm. The size obtained from XRD pattern is the grain size, while the size observed from the TEM image is the particle size. Since one particle may contain one or several grains, therefore, the size obtained from the TEM image can be greater than that calculated from XRD pattern. From the HRTEM image (Fig. 1B(ii)), it is obvious that the surface in an individual $\gamma\text{-Fe}_2\text{O}_3$ NPs is single crystalline with a lattice fringe spacing of 0.27 nm corresponding to (3 1 1) plane. The corresponding Fast Fourier Transform (Live FFT) image (Fig. 1B(iii)) also supports the single-crystalline nature of the $\gamma\text{-Fe}_2\text{O}_3$ NPs.

3.2. Peroxidase-like behavior of $\gamma\text{-Fe}_2\text{O}_3$ NPs

Peroxidase-like behavior of the as-synthesized $\gamma\text{-Fe}_2\text{O}_3$ NPs was investigated spectrophotometrically through the catalytic oxidation of a peroxidase substrate, TMB, in presence of H_2O_2 . This catalytic reaction was monitored by measuring the augmentation of TMB absorbance at 653 nm (Fig. 2A) producing a blue colored product which is originated from the oxidation product of TMB. This behavior is similar to the phenomenon observed for the commonly

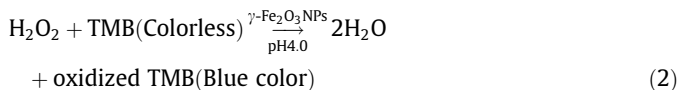
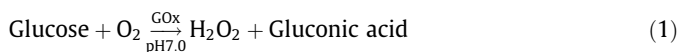
used horse radish peroxidase enzyme [20] and follows Michaelis-Menten kinetics (Fig. S2).

Another controlled experiments were carried out to compare the catalytic efficiency of the $\gamma\text{-Fe}_2\text{O}_3$ NPs by examining the time course process over 122 s run. Fig. 2B exhibits that the rate of the TMB- H_2O_2 - $\gamma\text{-Fe}_2\text{O}_3$ system is much higher than that of TMB- H_2O_2 system, whereas in presence of TMB- $\gamma\text{-Fe}_2\text{O}_3$ system, the rate is inferior. This indicates that the interactions among the nanoparticles, H_2O_2 and TMB are essential to enhance the catalytic process.

3.3. Colorimetric glucose estimation

On the basis of the intrinsic peroxidase-like property of the $\gamma\text{-Fe}_2\text{O}_3$ NPs i.e., TMB- H_2O_2 catalyzed color reaction; we have designed a colorimetric method for the detection and estimation of glucose which were easily understood by naked eye. When the above TMB- H_2O_2 catalytic reaction is coupled with the glucose catalytic reaction by glucose oxidase (GOx), the colorimetric detection of glucose could be eagerly understood because H_2O_2 is the main product of the GOx-catalyzed reaction.

In these cases, experiments need to be carried out in two steps viz. catalytic reaction of glucose with glucose oxidase (GOx) at pH 7.0 [phosphate buffer solution, (PBS) 10 mM, pH 7.0] (Eq.(1)), followed by the reaction of the liberated H_2O_2 with the peroxidase substrate, TMB, in presence of $\gamma\text{-Fe}_2\text{O}_3$ NPs at pH 4.0 (acetate buffer, 0.1 M, pH 4.0) (Eq.(2)) resulting in the development of a blue color (details in Supporting Information) as GOx is denatured in acidic condition.



Therefore, the color change for the oxidized TMB was employed to measure glucose content indirectly. Fig. 3 illustrates a typical absorbance (at 653 nm) versus glucose concentration response plot, where the response is linearly correlated to glucose concentration from 1 μM to 80 μM with a detection limit of 0.21 μM (signal to noise ratio = 3). These analytical results are also compared with several previously reported glucose sensors [24–29,32] in Table 1 and it can be concluded that the $\gamma\text{-Fe}_2\text{O}_3$ NPs shows either comparable or even better response towards glucose.

3.4. Mechanism of the reactions involve in glucose determination process

The glucose catalytic reaction may originate from the generation of hydroxyl radical (OH^\cdot) from the decomposition of H_2O_2 . Actually, the glucose determination reaction is performed in two steps-in the first step, the glucose is oxidized by dissolved oxygen in presence of GOx (Eq. (3)) to produce H_2O_2 while in the second step this H_2O_2 oxidizes the TMB substrate in presence of NPs:

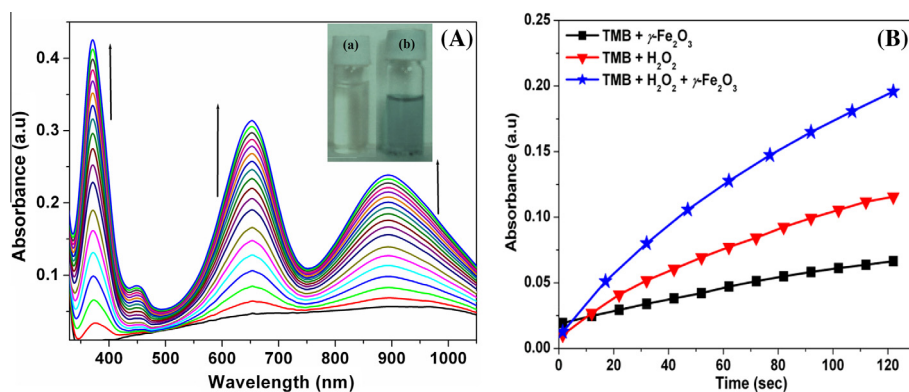


Fig. 2. (A) Time dependent UV-Vis spectral changes of TMB- H_2O_2 system catalyzed by $\gamma\text{-Fe}_2\text{O}_3$ NPs. Inset: Typical photography of TMB reaction system (a) with only catalyst NPs (colorless), (b) with H_2O_2 , after catalytic reaction in presence of NPs (blue color) (B) UV-Vis absorption-time course curve of TMB using $\gamma\text{-Fe}_2\text{O}_3$ NPs under different conditions. (For interpretation of the references to color in this figure legend, the reader is referred to the web version of this article.)

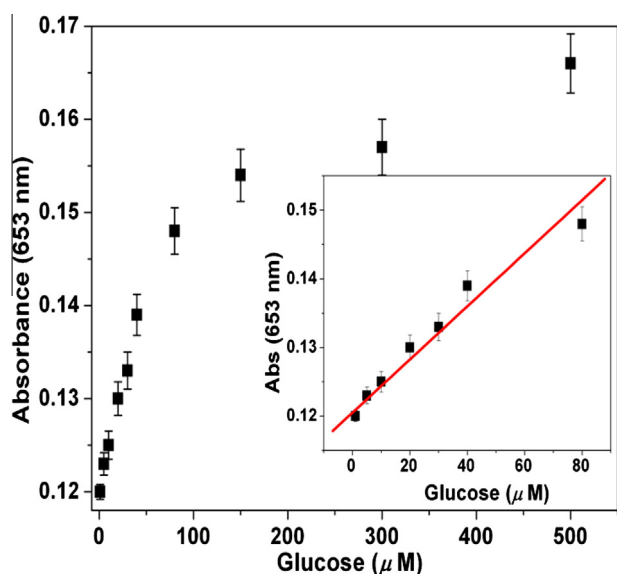


Fig. 3. Glucose concentration-response curve for glucose detection using GOx/TMB/ $\gamma\text{-Fe}_2\text{O}_3$ system. Inset: corresponding linear calibration plot for glucose. Error bar represent the standard deviation of three measurements.

Table 1

Comparison of glucose response parameters for $\gamma\text{-Fe}_2\text{O}_3$ NPs with other glucose sensors.

Catalyst	Linear range (μM)	Detection limit (μM)	Refs.
$\gamma\text{-Fe}_2\text{O}_3$ NPs	1–80 μM	0.21	This work
Carboxyl-modified graphene oxide	1–20	1	[24]
Fe_3O_4 nanoparticles	50–1000	30	[25]
Graphene oxide- Fe_3O_4	2–200	0.74	[26]
CoFe layered double hydroxide (CoFe-LDHs) nanoplates	1–10	0.6	[27]
Gold nanoparticles	18–1100	4	[28]
AuNPs (H_2O_2 triggered sol-gel transition)	0–131	1	[29]
FeSe film	2–30	0.5	[32]

During the second step, the H_2O_2 molecules were adsorbed on the surface of $\gamma\text{-Fe}_2\text{O}_3$ NPs and then activated by the bound Fe^{2+} ion to generate the OH^\cdot (Eq. (4)), and the generated OH^\cdot was stabilized by $\gamma\text{-Fe}_2\text{O}_3$ NPs via partial electron exchange interaction [33]. TMB was then quantitatively oxidized by OH^\cdot to form a blue color product according to Eq. (5).

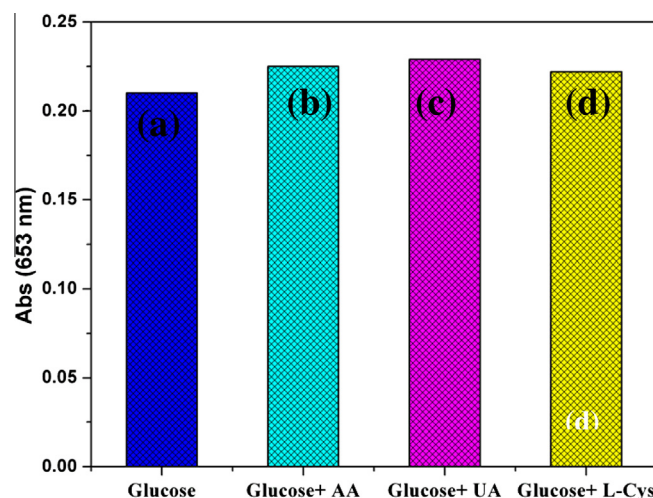
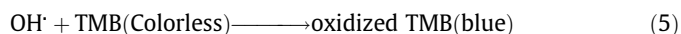


Fig. 4. During interference study, the corresponding bar diagram for the spectrophotometric response of TMB at 653 nm in presence of GOx for the addition of (a) 0.5 mM glucose only, (b) 0.5 mM glucose + 5 mM ascorbic acid, (c) 0.5 mM glucose + 5 mM uric acid and (d) 0.5 mM glucose + 5 mM L-cysteine.



The formation of OH^\cdot was confirmed by terephthalic acid (TA) photoluminescence probing techniques, which is highly sensitive and selective method and widely used in detection of hydroxyl radicals [31]. In presence of glucose reacting system, non-luminescent terephthalic acid reacted with OH^\cdot to produce strongly luminescent 2-hydroxy terephthalic acid (HTA) according He et al. [34] (Eq.(6)).

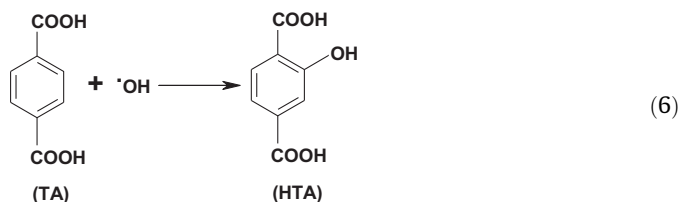


Table 2

Determination of glucose in real samples.

Sample	Pharmacopoeia method	Colorimetric method
Serum 1	5.94 mM (107.0 mg/dl) (GOD-POD method)	6.21 mM (112.0 mg/dl)
Serum 2	5.16 mM (93.0 mg/dl) (Hexokinase method)	5.38 mM (97.0 mg/dl)
Urine 1	4.91 mM (88.46 mg/dl) (Hexokinase method)	4.73 mM (85.22 mg/dl)
Urine 2	5.23 mM (94.23 mg/dl) (Hexokinase method)	5.06 mM (91.17 mg/dl)

Fig. S4 shows that the addition of different amount of γ -Fe₂O₃ NPs to a solution of glucose–GOx/TA at pH 7.0, where the fluorescence intensity of the solution ($\lambda_{\text{max}} = 425$ nm for HTA) increases continuously as the concentration of the γ -Fe₂O₃ NPs increased. This phenomenon suggests that the amount of generated $\cdot\text{OH}$ is also increased. However, there was no fluorescence intensity observed in the absence of Glucose/GOx system (Fig. S4). These results indicated that γ -Fe₂O₃ NPs could decompose in situ formation of H₂O₂ from Glucose/GOx system to generate the $\cdot\text{OH}$ radical.

3.5. Interference study of the γ -Fe₂O₃ bio-sensor

One of the most important analytical factors for a biosensor is the selectivity of the sensor to target analyte. It is well known that, some electro-active species in serum such as ascorbic acid (AA), uric acid (UA), L-cysteine (L-Cys) may influence the performance of glucose biosensor. Therefore, the selectivity and anti-interference ability of the biosensor was investigated by addition of specified amount UA (5 mM), AA (5 mM) and L-Cys (5 mM) during the spectrophotometric response measurement of 0.5 mM glucose. The corresponding bar diagram for the intensities of absorbance at 653 nm for all samples is shown in Fig. 4. No obvious absorbance responses were observed with the addition of certain amount of those electro-active interfering chemicals even if the concentration is increased up to 10-fold than that of glucose. All these observations indicate that the proposed glucose biosensor has high selectivity towards glucose i.e., good anti-interference ability.

3.6. The stability and reproducibility of the γ -Fe₂O₃ bio-sensor

The reproducibility of the proposed bio-sensor was studied by adding a fixed amount of glucose (50 μM) to PBS (10 mM, pH 7.0) containing GOx and the reaction is coupled with the same TMB–H₂O₂ catalytic reaction. As the γ -Fe₂O₃ NPs is an inorganic material, therefore it is expected to be more thermally and chemically stable than HRP based glucose bio-sensor. The relative standard deviation (RSD) of the sensor response was 3.6% for five successive measurements for the same electrode. When the γ -Fe₂O₃ NPs were stored at 4 °C for 1 week, the spectrophotometric response remained 96% of its original value, suggesting the long-term stability of the electrode.

3.7. Real sample analysis

A literature survey reveals that a considerable amount of glucose is excreted in normal human urine [35,36]. Urine contains auto-oxidizable molecule, which on exposure to O₂, undergo rapid auto-oxidation reaction to generate H₂O₂. Therefore, an attempt has been made to determine the concentration of glucose in excreted human urine as well as a blood using the above glucose determination technique. Instead of glucose, the diluted human urine and serum samples were used with glucose oxidase (GOx) for glucose catalyzed reaction as stated above and the corresponding absorbance values were measured at a wavelength of 653 nm. According to the calibration curve, the concentration of glucose in

the normal human serum and urine samples agreed well with that measured through standard GOD-POD or hexokinase method in pathological laboratory (Table 2). This novel finding may allow γ -Fe₂O₃ NPs to become a new candidate for monitoring blood and urine glucose level in diabetic patients.

In summary, cubic γ -Fe₂O₃ NPs, with average crystal size of 30 nm, were investigated as an artificial peroxidase-mimic like HRP, which show high affinity to both TMB and H₂O₂ producing blue-colored reaction. Based on this catalyzed colored reaction, glucose has been estimated in the linear range from 1 to 80 μM with detection limit of 0.21 μM . It also possesses good reproducibility and long-term stability. Finally, we have measured blood glucose and urine glucose level of normal human volunteers through the same catalyzed colored-reaction in presence of γ -Fe₂O₃ NPs based sensor. All these studies suggest that our as-synthesized easily recoverable and environmental friendly γ -Fe₂O₃ NPs is attractive material which will facilitate the utilization in the field of medical diagnostic and biotechnology.

Acknowledgments

Authors are thankful to Prof. Bibhutoh Adhikary, Department of Chemistry, Indian Institute of Engineering Science and Technology, Shibpur for helpful suggestions during work and for preparation of the manuscript. A.K. Dutta is indebted to CSIR, India, for his R.A. [F. No. 08/003(96)/2013–EMR–I]. The authors also acknowledge Dr. Papu Biswas, Department of Chemistry, Indian Institute of Engineering Science and Technology, Shibpur for providing instrumental facility such as diode-array spectro-photometer. The authors acknowledge the facilities developed in the Department of Chemistry, BESUS through MHRD (India) and UGC-SAP (India).

Appendix A. Supplementary data

Supplementary data associated with this article can be found, in the online version, at <http://dx.doi.org/10.1016/j.bbrc.2014.07.028>.

References

- [1] Y. Xu, P.E. Pehrsson, L. Chen, R. Zhang, W. Zhao, J. Phys. Chem. C 111 (2007) 8638–8643.
- [2] C. Song, P.E. Pehrsson, W. Zhao, J. Mater. Res. 21 (2006) 2817–2823.
- [3] R. Badugu, J.R. Lakowicz, C.D. Geddes, Anal. Chem. 76 (2004) 610–618.
- [4] A. Heller, B. Feldman, Chem. Rev. 108 (2008) 2482–2505.
- [5] H.G. Rennke, B.D. Rose, Renal Pathophysiology–The Essentials, first ed., Lippincott Williams, Philadelphia, 1994, p. 194.
- [6] D. Corazon, C. Wilborn, Conjecture Corporation, 09 September, 2010c. <<http://www.wisegeek.com>>.
- [7] T. Saxl, F. Khan, D. Matthews, Z.L. Zhi, S. Ameer-Beg, O. Rolinski, J. Pickup, Biosens. Bioelectron. 24 (2009) 3229–3234.
- [8] H. Chung, M.A. Arnold, M. Rhiel, D.W. Murhammer, Appl. Spectrosc. 50 (1996) 270–276.
- [9] L. Yang, C. Du, X. Luo, J. Nanosci. Nanotechnol. 9 (2009) 2660–2663.
- [10] A.C. Mendes, M.M. Caldeira, C. Silva, S.C. Burgess, M.E. Merritt, F. Gomes, C. Barosa, T.C. Delgado, F. Franco, P. Monteiro, L. Providencia, J.G. Jones, Magn. Reson. Med. 56 (2006) 1121–1125.
- [11] L.A. Hammad, M.M. Saleh, M.V. Novotny, Y. Mechref, J. Am. Soc. Mass Spectrom. 20 (2009) 1224–1234.
- [12] A.P. Cook, T.M. MacLeod, J.D. Appleton, A.F. Fell, J. Clin. Pharm. Ther. 14 (2009) 189–195.

- [13] I. Rzygalinski, E. Pobozy, R. Drewnowska, M. Trojanowicz, *Electroanalysis* 29 (2008) 1741–1748.
- [14] J. Lewandowski, P.S. Malchesky, J. Krzymien, E. Szczepanskasadowska, M. Nalecz, Y. Nose, *IEEE Trans. Biomed. Eng.* 31 (1984) 582–590.
- [15] P. Benvenuto, A.K.M. Kafi, A. Chen, *J. Electroanal. Chem.* 627 (2009) 76–81.
- [16] Y.G. Zhou, S. Yang, Q.Y. Qian, X.H. Xia, *Electrochem. Commun.* 11 (2009) 216–219.
- [17] J. Wang, D.F. Thomas, A. Chen, *Anal. Chem.* 80 (2008) 997–1004.
- [18] R.T. Kachosangi, G.G. Wildgoose, R.G. Compton, *Analyst* 133 (2008) 888–895.
- [19] P. Holt-Hindle, S. Nigro, M. Asmussen, A. Chen, *Electrochem. Commun.* 10 (2008) 1438–1441.
- [20] L. Gao, J. Zhuang, L. Nie, J.B. Zhang, Y. Zhang, N. Gu, T.H. Wang, J. Feng, D.L. Yang, S. Perrett, X.Y. Yan, *Nat. Nanotechnol.* 2 (2007) 577–583.
- [21] V. Sanz, S. de Marcos, J.R. Castillo, J. Galban, *J. Am. Chem. Soc.* 127 (2005) 1038–1048.
- [22] M. Morikawa, N. Kimizuka, M. Yoshihara, T. Endo, *Chem. Eur. J.* 8 (24) (2002) 5580–5584.
- [23] J. Tkac, T. Ruzgas, *Electrochem. Commun.* 8 (2006) 899–903.
- [24] Y.J. Song, K.G. Qu, C. Zhao, J.S. Ren, X.G. Qu, *Adv. Mater.* 22 (2010) 2206–2210.
- [25] H. Wei, E. Wang, *Anal. Chem.* 80 (2008) 2250–2254.
- [26] Y. Dong, H. Zhang, Z.U. Rahman, L. Su, X. Chen, J. Hu, X. Chen, *Nanoscale* 4 (2012) 3969–3976.
- [27] Y. Zhang, J. Tian, S. Liu, L. Wang, X. Qin, W. Lu, G. Chang, Y. Luo, A.M. Asiri, A.O. Al-Youbi, X. Sun, *Analyst* 137 (2012) 1325–1328.
- [28] R. Gill, L. Bahshi, R. Freeman, I. Willner, *Angew. Chem. Int. Ed.* 47 (2008) 1676–1683.
- [29] C. Xu, J. Ren, L. Feng, X. Qu, *Chem. Commun.* 48 (2012) 3739–3741.
- [30] A.K. Dutta, S.K. Maji, D.N. Srivastava, A. Mondal, P. Biswas, P. Paul, B. Adhikary, *J. Mol. Catal. A Chem.* 360 (2012) 71–77.
- [31] J.C. Barreto, G.S. Smith, N.H.P. Strobel, P.A. McQuillin, T.A. Miller, *Life Sci.* 56 (1995) 89–96.
- [32] A.K. Dutta, S.K. Maji, A. Mondal, B. Karmakar, P. Biswas, B. Adhikary, *Sens. Actuators B Chem.* 173 (2012) 724–731.
- [33] W. Shi, X. Zhang, S. He, Y. Huang, *Chem. Commun.* 47 (2011) 10785–10787.
- [34] Y. He, D. Li, G. Xiao, W. Chen, Y. Chen, M. Sun, H. Huang, X. Fu, *J. Phys. Chem. C* 113 (2009) 5254–5262.
- [35] T. Urakami, J. Suzuki, A. Yoshida, H. Saito, H. Mugishima, *Diabetes Res. Clin. Pract.* 80 (2008) 473–476.
- [36] C. Radhakumary, K. Sreenivasan, *Anal. Chem.* 83 (2011) 2829–2833.